Identification of Major Tyrosine Phosphorylation Sites in the Human Insulin Receptor Substrate Gab-1 by Insulin Receptor Kinase in Vitro†

Stefan Lehr,§ Jörg Kotzka,§ Armin Herkner,§ Albert Sikmann,‡ Helmut E. Meyer,‡ Wilhelm Krone,§ and Dirk Müller-Wieland*,§

Klinik II und Poliklinik für Innere Medizin at the Centre of Molecular Medicine of Cologne, Universität zu Köln, Cologne, Germany, and Proteinstrukturlabor der Ruhr-Universität Bochum, Germany

Received April 28, 2000; Revised Manuscript Received June 21, 2000

ABSTRACT: Gab-1 (Grb2-associated binder-1), which appears to play a central role in cellular growth response, transformation, and apoptosis, is a member of the insulin receptor substrate (IRS) family. IRS proteins act downstream in the signaling pathways of different receptor tyrosine kinases, including the insulin receptor (IR). In this paper, we characterize the phosphorylation of recombinant human Gab-1 (hGab-1) by IR in vitro. Kinetic phosphorylation data revealed that hGab-1 is a high affinity substrate for the IR (K_M: 12.0 μM for native IR vs 23.3 μM for recombinant IR). To elucidate the IR-specific phosphorylation pattern of hGab-1, we used phosphopeptide mapping by two-dimensional HPLC analysis. Phosphorylated tyrosine residues were subsequently identified by sequencing the separated phosphopeptides by matrix assisted laser desorption ionization mass spectrometry (MALDI-MS) and Edman degradation. Our results demonstrate that hGab-1 was phosphorylated by IR at eight tyrosine residues (Y242, Y285, Y373, Y447, Y472, Y619, Y657, and Y689). Seventy-five percent of the identified radioactivity was incorporated into tyrosine residues Y447, Y472, and Y619 exhibiting features (NYVPM motif) of potential binding sites for the regulatory subunit (p85) of phosphatidylinositol (PI)-3 kinase. Accordingly, pull down assays with human HepG2 cell lysates showed that IR-specific phosphorylation of wild-type hGab-1 strongly enhanced PI-3 kinase binding. This is still the case when a single tyrosine residue in the NYVPM motif was mutated to phenylalanine. In contrast, phosphorylation-dependent binding of PI-3 kinase was completely abolished by changing a second tyrosine residue in a NYVPM motif independent from its location. Recently, we identified a similar cohort of tyrosine phosphorylation sites for the epidermal growth factor receptor (EGFR) with a predominant phosphorylation of tyrosine residue Y657 and binding of Syp [Lehr, S. et al. (1999) *Biochemistry 38*, 151−159]. These differences in the phosphorylation pattern of hGab-1 may contribute to signaling specificity by different tyrosine kinase receptors engaging distinct SH2 signaling molecules.

Various intracellular signaling pathways are activated by receptor tyrosine kinases (RTKs)[1] (*2*). To understand the molecular basis of cell signaling specificity, the nature of each pathway has to be uncovered. A common feature of RTK signaling is recruiting intracellular adapter proteins such as Gab-1. Gab-1 is phosphorylated after stimulation of cells by insulin and several other growth factors, such as the nerve growth factor (NGF) (*3*), basic fibroblast growth factor (FGF) (*4*), hepatocyte growth factor (HGF) (*5*), and epidermal growth factor (EGF) (*6*) as well as by different cytokine and antigen receptors (*7*). Therefore, Gab-1 is involved in various intracellular signaling pathways; for example, NGF plays an important role in the maturation of the nervous system (*8*), whereas HGF activates cell proliferation, survival, motility, invasion of extracellular matrixes, and branched morphogenesis (*9*, *10*). In addition, a recent study with transgenic mice show that HGF is also a regulator of islet cell growth and differentiation indicating a link to diabetes mellitus (*11*).

Gab-1 (Grb2-associated binder-1) was originally cloned as a Grb2-associated protein from a human glia tumor expression library (*6*). Structural and functional features of Gab-1 indicate that it belongs to the multifunctional docking protein family consisting of the insulin receptor substrates (IRS1−4) and Gab-2 (for recent review, see refs *12* and *13*). Gab-1 contains a N-terminal PH domain, two SH3-binding

† This study was supported by the German Research Foundation (DFG/SFB-351; DFG/ME 765/3-4), Fritz Thyssen Stiftung, the German Ministry of Education and Research (BMBF/ 01 KS 9502), and by the Graduierten Kolleg (Molekulare Grundlagen pathophysiologischer Vorgänge; DFG) to S.L.

* To whom correspondence should be addressed: Dirk Müller-Wieland, MD, Klinik II und Poliklinik für Innere Medizin der Universität zu Köln 50924 Cologne, Germany. Telephone: +49-221-478-4070. Fax: +49-221-478-4179. E-mail: dirk.mueller-wieland@medizin.uni-koeln.de.

‡ Proteinstrukturlabor der Ruhr-Universität Bochum.

§ Universität zu Köln.

[1] Abbreviations: PLC-γ, phospholipase Cγ; EGFR, epidermal growth factor receptor; FGF, fibroblast growth factor; Gab-1, Grb2-associated binder-1; GST, glutathione-*S*-transferase; HGF, hepatocyte growth factor; HepG2, human hepatoma cells; HPLC, high performance liquid chromatography; IR, insulin receptor; IRS, insulin receptor substrate; IL4, interleukin 4; MALDI-MS, matrix assisted laser desorption ionization mass spectrometry; NGF, nerve growth factor; p85, regulatory subunit of phosphatidylinositol (PI)-3 kinase; PAGE, polyacrylamide gel electrophoresis; PDGF, platelet derived growth factor receptor; PSD, post source decay; RP, reversed phase; RTKs, receptor tyrosine kinases; SH2, src-homology domain 2; WGA, wheat germ agglutinine.

10.1021/bi000982k CCC: $19.00
Published on Web 08/04/2000

proline-rich regions, and 47 potential serine as well as 17 potential tyrosine phosphorylation sites that represent Src homology 2 (SH2)-binding motifs. Accordingly, phosphorylated Gab-1 recruits downstream signaling elements possessing SH2-domains, such as the regulatory subunit (p85) of the phosphatidylinositol (PI)-3 kinase, phospholipase Cγ (PLC-γ), the protein tyrosine phosphatase Syp (*6*), and Crk (*7*) in various cell systems.

As a consequence of these and other interactions, the IRS proteins mediate downstream effects, including direct activation of PI-3 kinase and Syp. Therefore, intracellular signaling appears to be determined by a complex network of protein−protein interactions regulated by tyrosine phosphorylation.

Hence the multifunctional adapter protein Gab-1 appears to integrate different extracellular stimuli recruiting various intracellular signaling proteins. Generation of signaling selectivity by recruiting docking proteins at the molecular level might be controlled by phosphorylation of specific tyrosine residues with different RTKs. Recently, we have shown that Gab-1 is specifically phosphorylated on eight tyrosine residues by the EGFR. Tyrosine Y657 in the C-terminal domain turned out to be the major phosphorylation site mediating a single specific interaction of hGab-1 and Syp (*1*).

In this paper, we show the identification of tyrosine phosphorylation sites in human Gab-1 (hGab-1) related to the IR in vitro. Signaling selectivity appears not to be determined only by different phosphorylation sites but rather corresponds to the amount of phosphorylation of single tyrosine residues.

EXPERIMENTAL PROCEDURES

Construction and Expression of Human Recombinant GST-Fusion Protein. Human Grb2-associated binder-1 (hGab-1)-GST fusion protein (aa 1 to 724 with apparent molecular mass = 105.6 kDa) was prepared as previously described (*1*).

Insulin Receptor (IR) Kinase Preparation. Human hepatoma cells (HepG2) were cultured at 37 °C, 5% CO_2 (v/v), in RPMI 1640 medium supplemented with 10% fetal bovine serum and antibiotics (Life Technologies, Inc.). For receptor preparation, HepG2 cells were incubated for 24 h in serum-starved medium before receptor purification by wheat germ agglutinine (WGA) (*14*).

Substrate Phosphorylation Assay. For GST-fusion protein phosphorylation by recombinant receptor kinase domaine, rIR (Stratagene) was autophosphorylated for 5 min at 22 °C in kinase buffer [50 mM HEPES/NaOH (pH 7.5), 5 mM $MgCl_2$, 5 mM $MnCl_2$, 1 mM DTT, 1 mM Na_3VO_4, 1 μM poly(lysine), 250 μM ATP, 0.1 mCi/mL [γ-^{32}P]ATP, and 1 mg/mL BSA]. Substrate phosphorylation subsequently was initiated by addition of autophosphorylated recombinant receptors (2.5 pmol) to aliquots of hGab-1 in kinase buffer resulting in substrate concentrations ranging from 0.25 to 32 μM. The reaction proceeded for 60 s at 22 °C and was terminated by addition of 2× sample buffer (50 mM Tris/HCl, pH 6.8, 100 mM DTT, 10% glycerol, 2% SDS, and 0.1% bromphenol blue) followed by boiling for 5 min. Phosphorylated proteins were separated by 10% SDS−PAGE (*15*) and analyzed by autoradiography of the Coomassie stained and dried gels. Phosphate incorporations were determined by counting Cerenkov radiation of gel slices.

To phosphorylate substrate by WGA-purified receptors, WGA-column eluted protein was preincubated for 60 min at 4 °C with 10 nM insulin in kinase buffer supplemented with 0.1% Triton X-100. Autophosphorylation was carried out for 10 min at 22 °C as described above. Substrate phosphorylation subsequently was initiated by the addition of autophosphorylated receptors (equivalent to 2.5 μg of WGA eluted protein) to aliquots of hGab-1 in kinase buffer resulting in substrate concentrations of 0.25−64 μM, respectively. Reaction proceeded for 180 s at 22 °C. Subsequent sample preparation was performed as described above.

Conversion of protein concentration into molar units was based on the calculated molecular mass of the GST fusion proteins. The K_M values were determined using the Enzfitter program (Elsevier, Biosoft).

High Performance Liquid Chromatography (HPLC) and Matrix Assisted Laser Desorption Ionization Mass Spectrometry (MALDI-MS). Using 0.3 nmol of rIR, 5 nmol of Gab-1 protein was phosphorylated with [γ-^{32}P]ATP for 25 min under conditions described above. The proteins were separated by SDS−PAGE, and phosphorylated hGab-1 was digested with 50 μg trypsin (sequencing grade, Roche) in the excised gel pieces overnight at 37 °C (*16*, *17*). The peptides were eluted with 50 mM ammonium carbonate and separated on an anion exchange column (Nucleogel SAX 1000-8/46, 50 × 4.6 mm, Machery & Nagel) using Beckmann gold solvent delivery system. The HPLC flow rate was 0.5 mL/min. After injection of 1 mL of sample, the peptides were eluted beginning at 100% buffer A (20 mM NH_4CH_2-COOH, pH 7.0) and 0% of buffer B (0.5 M KH_2PO_4, pH 4.0). The amount of buffer B was increased to 10% within 40 min and from 10 to 50% during the following 75 min. Fractions of 0.5 mL were collected. Radioactive fractions from rIR-catalyzed phosphorylation of hGab-1 were subjected to reversed phase HPLC. The peptides were separated on C18-reversed phase column (150 × 0.8 mm, 5 μm particle size, 300 A pore size, LC Packings, The Netherlands) using ABI 140 D solvent delivery system (Applied Biosystems, USA). The HPLC flow rate was adjusted to 15 μL/min. After application of 100 μL sample elution started with 95% of solution A (0.08% TFA) and 5% of solution B [acetonitrile/water/TFA (84/16/0.08; v/v/v)]. The content of solution B was raised to 50% in 90 min and from 50 to 100% in 15 min. Aliquots of the collected fractions were taken for measuring the radioactivity. Fractions containing radiolabeled peptides were subjected to Edman degradation with an Applied Biosystems model 494 cLc pulse-liquid sequenator (*18*) and MALDI-TOF mass spectrometry. For MALDI mass spectrometry, 0.5 μL of each selected fraction was directly prepared onto the MALDI target with a saturated solution of α-cyano-4-hydroxy-cinnamic acid in acetonitrile/0.1% TFA (1:1). Mass spectrometry was performed on a REFLEX III system (Bruker Daltonik, Bremen) equipped with a SCOUT 384 multiprobe ion source. Positive ion mass spectra were acquired in a linear and reflector mode using an acceleration voltage of 20 000 V. In addition to manual interpretation of PSD (post source decay) fragment ion spectra, the SEQUEST algorithm (OWL sequence database; University of Leeds) was used to identify the peptide phosphorylation sites (*19*, *20*).

Cellular Fractions. HepG2 cells were cultured as described above. After incubation for 24 h with serum-starved medium,

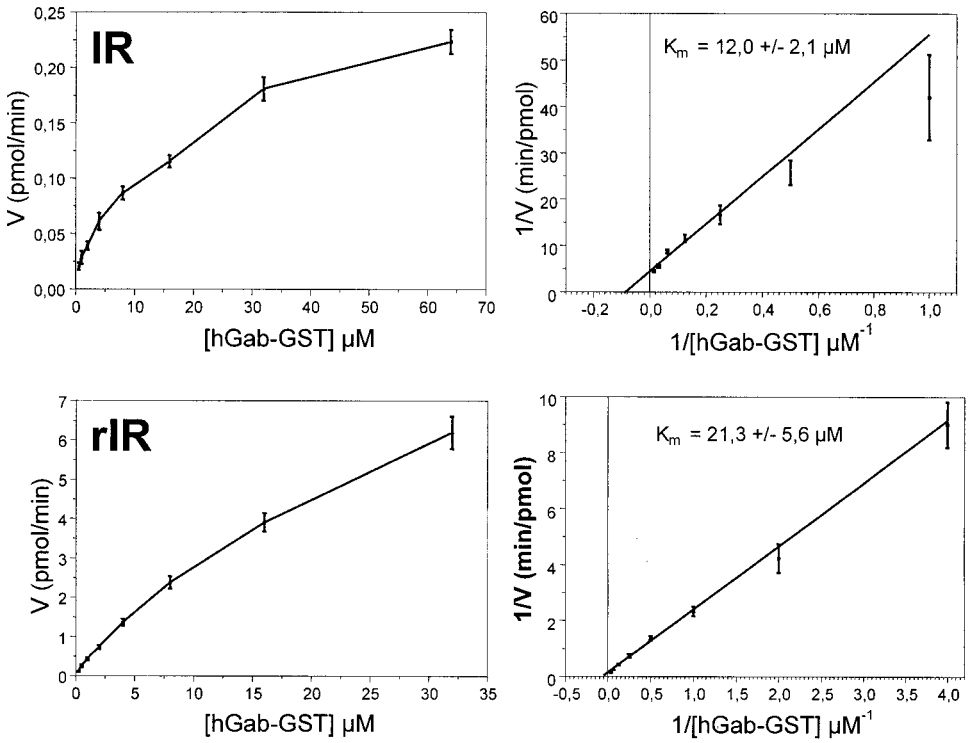

FIGURE 1: Michaelis−Menten kinetics of hGab-1 by IR. Phosphorylation of hGab-1 catalyzed by recombinamt insulin receptor kinase domain (rIR) and WGA-purified native insulin receptor (IR) is shown. Velocity (v) versus substrate concentration and double-reciprocal plots are shown. Mean values ±SD of four independent experiments are depicted in the plots. Methods used for phosphorylation reactions and determination of K_M values are described in Experimental Procedures.

the cells were washed twice with PBS. Cells were lysed in pull down (PD) buffer [50 mM Hepes, pH 7.5, 1% (v/v) Nonidet P-40, 150 mM NaCl, 5 mM EDTA, 10 mM NaF, 1mM Na_3VO_4, 1 mM glycerophosphate supplemented with complete (Roche)]. Insoluble material of cell lysates were removed by centrifugation at 12000*g* for 10 min at 4 °C.

GST Pull Down Assay. In vitro phosphorylated hGab-1 proteins (5 μg), nonphosphorylated hGab-1 proteins (5 μg), and GST (5 μg) were incubated with HepG2 lysates (1 mg each) for 30 min at 4 °C. Glutathion sepharose beads [50 μL of a 50% (v/v) slurry; APbiotech] were added, and samples were incubated at 4 °C on a rotator (60 rpm) for 1 h. Pellets were washed three times with PD buffer. Bound proteins were eluted with 40 μL of 1× SDS−PAGE sample buffer and separated by SDS−PAGE.

SDS−PAGE and Western Blotting. SDS−PAGE was performed according to Laemmli (*15*) followed by electroblotting (*21*) to PVDF membranes (BioRad) for probing with antibodies detected by ECL (Amersham). The following primary antibodies were used in the suppliers recommended concentrations: antiphosphotyrosine monoclonal (RC20), anti-PI-3 kinase monoclonal (Transduction Laboratories), and anti-Gab-1 monoclonal (Upstate Biotechnology). Kodak X omat AR film was used for detection of chemiluminescence signals. Before reprobing, blots were incubated with stripping solution (100 mM 2-mercaptoethanol, 2% SDS, TBS) at 55 °C for 60 min. The washed blots were reblocked prior to reprobing.

Site-Directed Mutagenesis. The Tyr 447 → Phe 447, Tyr 472 → Phe 472, and Tyr 619 → Phe 619 mutants of hGab-1 as well as the corresponding multiple mutants (Tyr 447, 472 → Phe 447, 472; Tyr 447, 619 → Phe 447, 619; Tyr 472, 619 → Phe 472, 619; Tyr 447, 472, 619 → Phe 447, 472, 619) were made by site-directed mutagenesis using the QuickChange site-directed mutagenesis kit (Stratagene) according to the manufacturer's recommendations. The following primers were used: Tyr 447 → Phe 447 (5′-CTGGATGAAAATT**T**CGTCCCAATGAATCCC); Tyr 472 → Phe 472 (5′- CAGGAAGCAAATT**T**TGTGCCAATGACTCCAG G); Tyr 619 → Phe 619 (5′- GTGAAGAGAATT**T**TGTTCCCATGAACCC).

RESULTS

Gab-1, a High Affinity Substrate of the IR. To examine tyrosine phosphorylation of hGab-1 by the IR, we expressed hGab-1 as glutathione-*S*-transferase (GST) fusion protein as previously described (*1*). To perform substrate phosphorylation, we used the native insulin receptor (IR) as well as the soluble insulin receptor kinase (rIR), which is a common model for the human insulin receptor (IR) (*22*−*24*). hGab-1 is substantially phosphorylated by both receptor preparations (K_M: 12.0 ± 2.1 μM for WGA IR vs 23.3 ± 5.6 μM for rIR) in vitro, displaying comparable catalytic properties. Kinetic data of phosphorylated hGab-1 are shown in Figure 1. Phosphoamino acid analysis revealed phosphorylation exclusively on tyrosine residues (data not shown).

Identification of IR-Specific Tyrosine Phosphorylation Sites in hGab-1. hGab-1 is rapidly phosphorylated by the activated IR. To identify the IR-specific tyrosine phosphorylation sites of hGab-1 in vitro tryptic peptides obtained from rIR-phosphorylated [^{32}P]hGab-1 (5 nmol) were separated by anion exchange HPC. About 90% of the radioactivity was recovered from the gel after digestion, and between 80 and 90% of the radioactive peptides were eluted from the column. The radioactivity profile analyzed by anion exchange HPLC

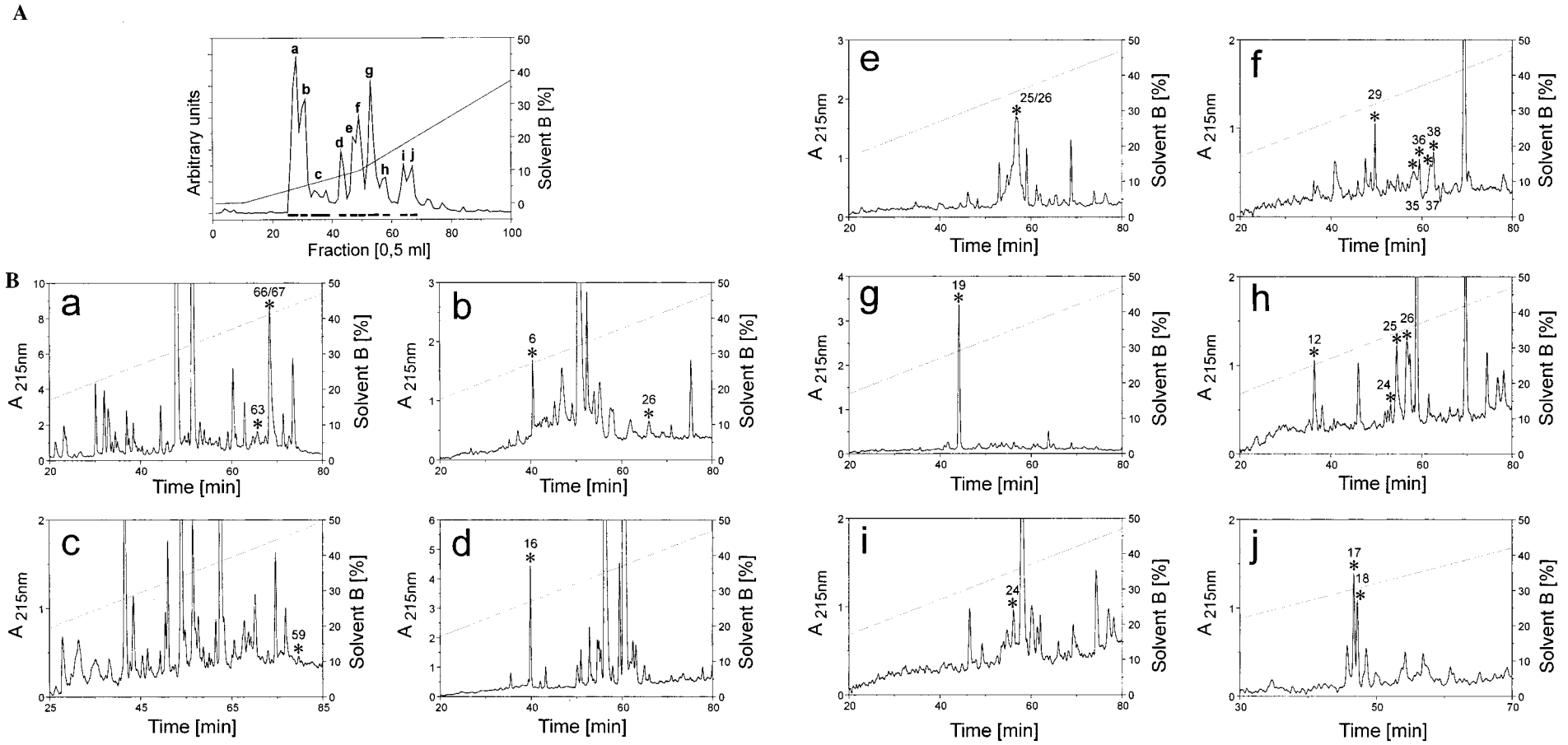

FIGURE 2: HPLC analysis of tryptic phosphopeptides derived from hGab-1 phosphorylated by rIR. *(*A) HPLC anion exchange chromatography of trypsinized hGab-1 phosphorylated by IR. Five nanomoles of hGab-1 were phosphorylated for 25 min with 0.3 nmol of rIR. The phosphorylation reaction was performed as described in Experimental Procedures. Proteins were separated by SDS−PAGE, and the excised hGab-1 was digested with trypsin. Radioactive fractions were pooled according to the solid bars. Pooled fractions a−j were subjected for rechromatography to C18 reversed phase HPLC. (B) a−j, reversed phase HPLC elution profiles of anion exchange HPLC fractions a−j are shown. Radioactive fractions are designated with asterisks followed by the fraction number.

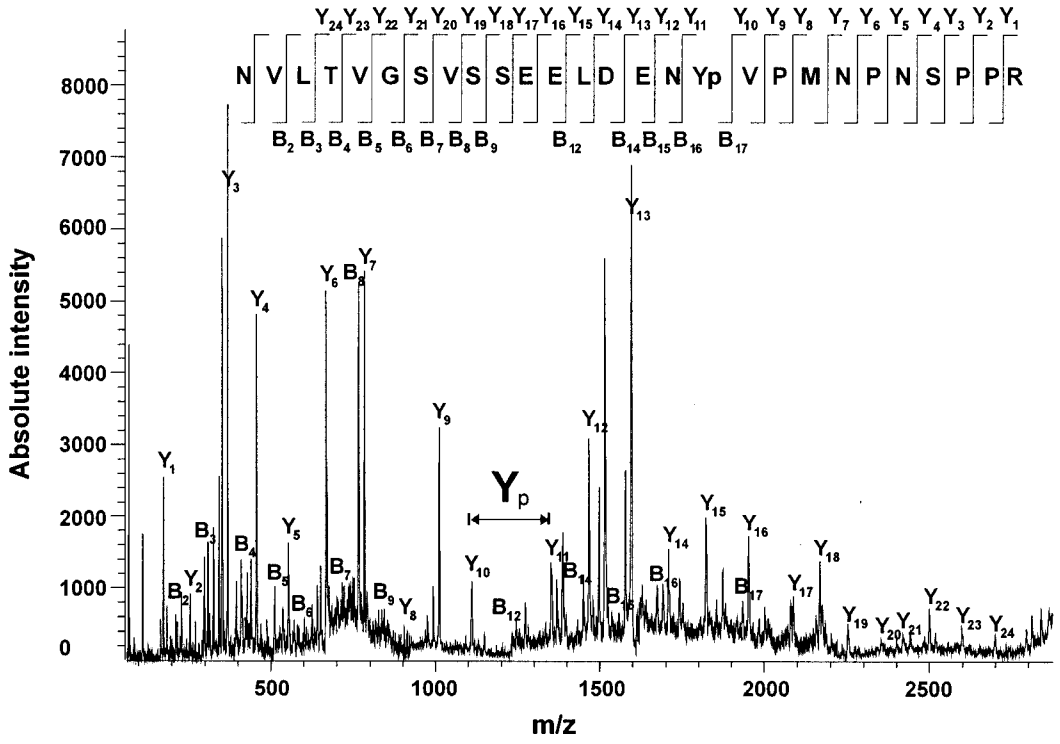


```
psd.851a.out
SEQUEST v.C1, Copyright 1993-96
Molecular Biotechnology, Univ. of Washington, J.Eng/J.Yates
Licensed to Finnigan MAT
02/23/99, 08:18 AM, 51 sec. on REFLEX-PC
mass=3024.4(+1), fragment_tol=1.00, mass_tol=0.10, MONO
# amino acids = 93015641, # proteins = 290104, # matched peptides = 332569
immonium (HFYWM) = (00000), total_inten=8005.8, lowest_Sp=260.9
ion series nA nB nY ABCDVWXYZ: 0 1 1 0.0 1.0 0.0 0.0 0.0 0.0 0.0 1.0 0.0
rho=0.200, beta=0.075, top 10, D:\datenbanken\owl.r##
C=160.01 Y=243.06

 #   Rank/Sp  (M+H)+    Cn    deltCn  C*10^4    Sp     Ions  Reference            Peptide
---  -------  ------  ------  ------  ------   ----    ----  ---------------      -------
 1.   1 /  1  3024.4  1.0000  0.0000  5.2471  4033.7  37/52  owl||S68442          (K)NVLTVGSVSSEELDENY*VPMNPNSPPR
 2.   2 /155  3024.5  0.3638  0.6362  1.9088   333.2  15/54  owl||CET06E46        (A)GQNGECIGGTVEDIPNDCVIIISKPLII
 3.   3 / 49  3024.4  0.3536  0.6464  1.8554   409.9  18/58  owl||MTH1_MOUSE      (E)AAAPRDEADSQGELVRRSGCGGLSKSPGPV
 4.   4 / 57  3024.5  0.3353  0.6647  1.7594   402.8  18/50  owl||ARCA_MYCAR +3   (P)GREIDYITPARLDELLFSAILESHDA
               owl||ARCA_MYCHO ARGININE DEIMINASE (EC 3.5.3.6). - MYCOP
               owl||A41465 arginine deiminase (EC 3.5.3.6) - Mycoplasma
               owl||MAARDI MAARDI NID: g48705 - Mycoplasma arginini
 5.   5 / 96  3024.4  0.3178  0.6822  1.6678   365.7  16/54  owl||S39621          (G)CDSNGKLNNKSVILEGDREHSSGAQIPV
 6.   6 /257  3024.5  0.3119  0.6881  1.6364   303.9  16/54  owl||AB002322   +1   (L)GQSRLETAESKEKMALPPQEDATASPPR
               owl||AC0044931 AC004493 NID: g2996648 - human
 7.   7 / 67  3024.4  0.2984  0.7016  1.5659   390.5  17/52  owl||GSHB_ARATH +2   (E)TLIVGGQAVAVVYFRSGYTPNDHPSES
               owl||S68223 glutathione synthase (EC 6.3.2.3) 2 precurso
               owl||S62654 glutathione synthase (EC 6.3.2.3) 2, cytosol
 8.   8 /416  3024.5  0.2921  0.7079  1.5325   271.1  15/54  owl||YN83_CAEEL +1   (F)IVSKYGIETHSIGEDILVPAMSQVAVST
               owl||CEZC841 CEZC84 NID: g6927 - Caenorhabditis elegans
 9.   9 /316  3024.4  0.2919  0.7081  1.5314   289.6  16/50  owl||MNB_HUMAN  +3   (D)VNLTVYSNPRQETGIAGHPTYQFSAN
               owl||HSU58496 HSU58496 NID: g1381155 - human
               owl||MMU58497 MMU58497 NID: g1381157 - house mouse strai
               owl||RNPSK47 RNPSK47 NID: g2582815 - Norway rat
10.  10 / 15  3024.4  0.2909  0.7091  1.5266   482.1  17/48  owl||A64689          (H)VLNQESLNYSFGKLKDATIGESCYK

 1.  owl||S68442 Grb2-associated binder-1 protein - huma
 2.  owl||CET06E46 CET06E4 NID: g1262984 - Caenorhabditis elegans
 3.  owl||MTH1_MOUSE HELIX-LOOP-HELIX PROTEIN MATH-1. - MUS MUSCULUS (MOUSE)
```

FIGURE 3: Fragmentation mass spectrum of hGab-1 derived peptides containing PI-3 kinase binding motifs. MALDI analysis for the phosphopeptide of *m/z* 3024.4. The phosphotyrosine peptide NVLTVGSVSSEELDENY*$_{447}$VPMNPNSPPR (aa 431−457) was identified. Identified b- and y-fragment ions are designated. These PSD fragment data allowed identification of the phosphorylated amino acid residue in the known primary structure. Beneath the spectrum, the results of computer-aided SEQUEST analysis is shown. The top-ranked choice by SEQUEST corresponds to the manually determined peptide sequence.

of phosphorylated hGab-1 behaved independent from phosphorylation time up to 60 min (data not shown). This radioactivity (Cerenkov) elution profile (Figure 2A) showed 10 reproducible major peaks (a−j). To separate comigrating peptides, radioactive fractions of each peak were pooled according to the elution profile and subjected to reversed phase (RP)-HPLC (Figure 2B). This yielded 22 different radiolabeled RP-HPLC fractions that were subsequently subjected to MALDI mass spectrometry and measured in the reflector mode (MALDI-PSD). Locations of phosphotyrosine residues (Table 1) were confirmed by automated Edman degradation.

To elucidate the primary structure of the separated phosphopeptides, the corresponding parent ion masses were measured by MALDI-MS. Subsequently, PSD spectra of the respective parent ion masses were acquired. Figures 3−5 show MALDI-PSD spectra of the three hGab-1 phosphopeptides representing the major IR-specific phosphorylation sites. Fragment ions observed in the mass spectra were used for automated interpretation by the SEQUEST algorithm with

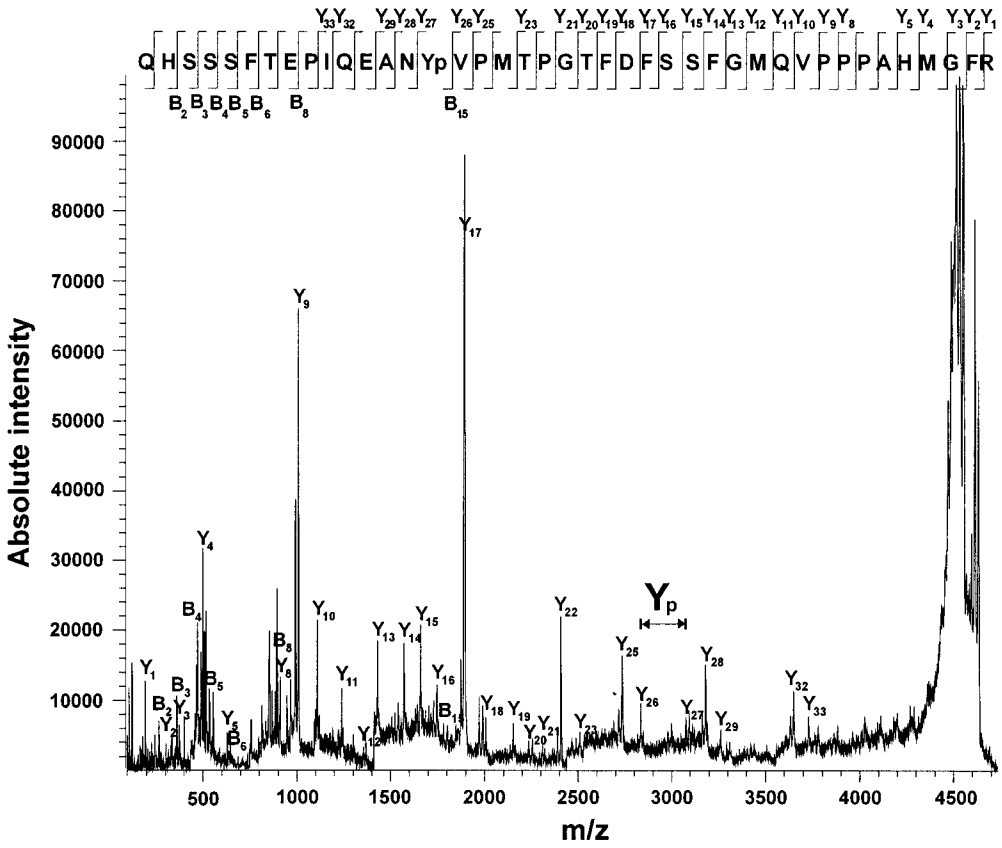


```
psd.864.out
SEQUEST v.C1, Copyright 1993-96
Molecular Biotechnology, Univ. of Washington, J.Eng/J.Yates
Licensed to Finnigan MAT
02/24/99, 07:13 PM, 1 min. 11 sec. on REFLEX-PC
mass=4636.2(+1), fragment_tol=1.20, mass_tol=1.00, MONO
# amino acids = 93015641, # proteins = 290104, # matched peptides = 20295
immonium (HFYWM) = (00000), total_inten=4596.0, lowest_Sp=19.8
ion series nA nB nY ABCDVWXYZ: 0 1 1 0.0 1.0 0.0 0.0 0.0 0.0 0.0 1.0 0.0
rho=0.200, beta=0.075, top 10, D:\datenbanken\owl.r##
C=174.01 Y=243.06 Enzyme:Trypsin 1 KR P
```

#	Rank/Sp	(M+H)+	Cn	deltCn	C*10^4	Sp	Ions	Reference		Peptide
1.	1 / 1	4637.0	1.0000	0.0000	1.6005	593.9	25/80	owl||S68442		(R)QHSSSFTEPIQEANY*VPMTPGTFDFSSFGMQVPPPAHMGFR
2.	2 /168	4635.4	0.5035	0.4965	0.8059	27.8	8/68	owl||TRHY_RABIT		(R)QEEQELRQERDRKLREEEQLLRQEEQELRQERDRK
3.	3 / 42	4635.2	0.4966	0.5034	0.7948	37.2	9/76	owl||JQ2034		(R)AESIARDCGGLSEVINLVARRLRRQYGVASEDEVPHYFK
4.	4 / 15	4636.3	0.4660	0.5340	0.7457	45.2	10/78	owl||LLU233761		(-)MVQENMKAFGTMAEKETPKTKETQPEIKGALTYEDKVVQK
5.	5 /286	4635.9	0.4373	0.5627	0.6999	23.7	7/78	owl||GHR_CHICK		(K)DDDSGRASCYEPDIPETDFSASDTCDAISDIDQFKKVTEK
6.	6 /207	4635.5	0.4366	0.5634	0.6988	26.3	9/92	owl||C70752		(R)HELADPLTPILAVGAAASAIVGSNIDALLVAGVMTVNAITGGVQRLR
7.	7 /388	4636.3	0.4352	0.5648	0.6965	21.6	7/86	owl||BSY171572		(K)IIGIDLGTTNSCVSVLEGGEPKVIPNPEGNRTTPSVVAFKNGER
8.	8 /241	4636.0	0.4210	0.5790	0.6738	24.9	6/76	owl||ATU49919	+1	(R)ENPSGDFRSMYRHISKGAWTFSDRDHGWQVSDCTAEALK
		owl||YUP8H12R40 YUP8H12R NID: g2494106 - thale cress								
9.	9 / 21	4635.4	0.4119	0.5881	0.6593	40.5	9/78	owl||PHS2_RABIT	+9	(R)TNFDAFPDKVAIQLNDTHPSLAIPELMRVLVDLERLDWDK
10.	10 /100	4637.1	0.4031	0.5969	0.6452	31.8	8/76	owl||POP1_SCHPO		(R)SLEEHEGDVWTFEYVGDTLVTGSTDRTVRVWDLRTGECK

1. owl||S68442 Grb2-associated binder-1 protein - huma
2. owl||TRHY_RABIT TRICHOHYALIN. - ORYCTOLAGUS CUNICULUS (RABBIT)
3. owl||JQ2034 RNA-directed RNA polymerase (EC 2.7.7.48) - beet cryptic virus

FIGURE 4: Fragmentation mass spectrum of hGab-1 derived peptides containing PI-3 kinase binding motifs. MALDI analysis for the phosphopeptide of m/z 4637.0. The phosphotyrosine peptide QHSSSFTEPIQEANY*$_{472}$VPMTPGTFDFSSFGMQVPPPAHMGFR (aa 458−498) was identified. Identified b- and y-fragment ions are designated. These PSD fragment data allowed identification of the phosphorylated amino acid residue in the known primary structure. Beneath the spectrum, the results of computer-aided SEQUEST analysis is shown. The top-ranked choice by SEQUEST corresponds to the manually determined peptide sequence.

a +80-Da modification specific for tyrosine residues. This leads to the identifcation of the phosphopeptide containing tyrosine Y_{447} (aa 431−457; NVLTV GSVSSEELDENY*$_{447}$-VPMNPNSPPR) (Figure 3) and Y_{472} (aa 458−498; QHSSS-FTEPI QEANY*$_{472}$VPMTPGTFDFSSFGMQVPPPAHMG-FR) (Figure 4). In addition, theoretical values of b- and y-type ions for these phosphopeptides were calculated and compared to the fragment ions observed in the mass spectra to confirm the sequence assignment. The positions of the phosphorylated tyrosine residue were identified within both the b- and y-ion series. PSD analysis of a phosphopeptide with the parent ion mass of 6186.6 Da achieved predominately internal fragment ion masses. Caused by the high peptide mass and the high amount of proline residues only weak a-, b-, y- or b-ions were observed in the PSD spectra. Analysis of these data lead to the identification of a phosphopeptide containing tyrosine residue Y_{619} (aa 594−648; FPMSPRPDSVHSTT-SSSDSHDSEENY*$_{619}$VPMNPNLSSEDPNL FGSNSLDGG-SSPMIK) (Figure 5). The position of the phosphorylated tyrosine residue was identified by comparing these internal fragment ion masses with the calculated theoretical masses and was confirmed by automated Edman degradation (data not shown).

Interestingly, over 75% of the radioactivity incorporated in the identified phosphopeptides could be associated with these three peptides. The identified phosphorylated tyrosine

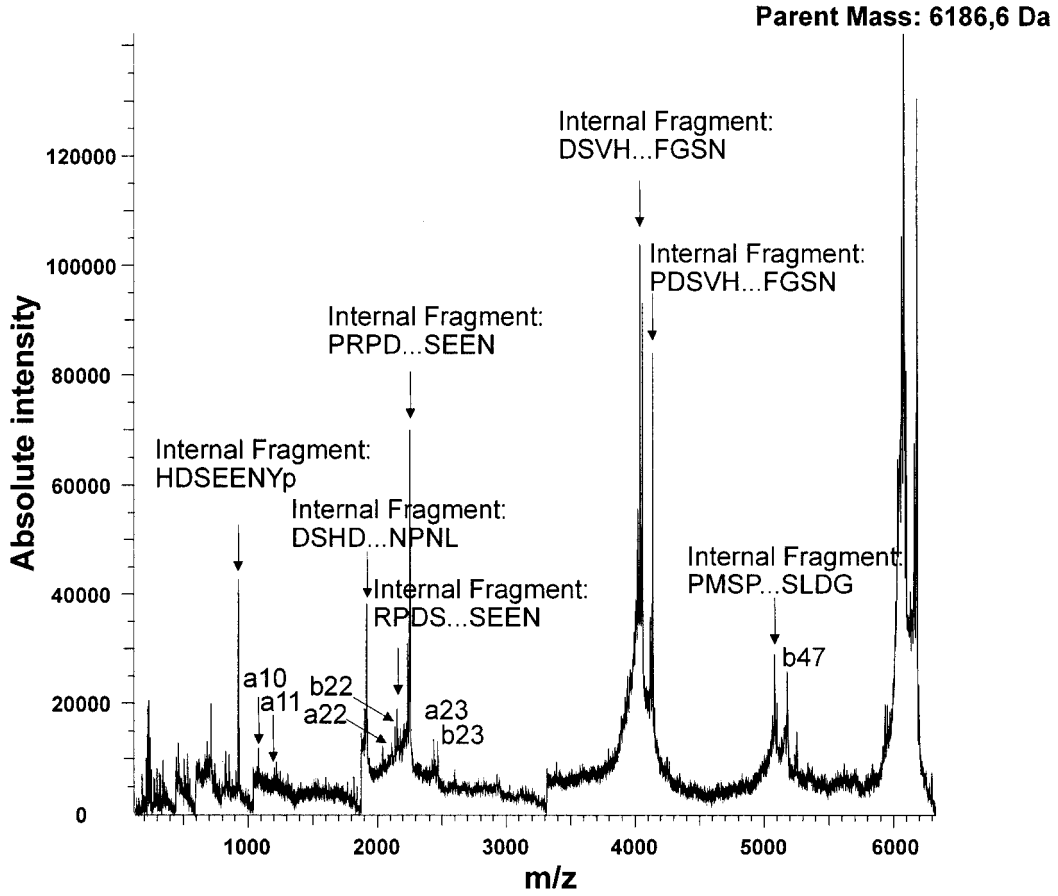

FIGURE 5: Fragmentation mass spectrum of hGab-1 derived peptides containing PI-3 kinase binding motifs. MALDI analysis for the phosphopeptide of *m/z* 6186.6. The phosphotyrosine peptide FPMSPRPDSVHSTTSSSDSHDSEENY*$_{619}$VPMNPNLSSEDPNLFGSN-SLDGGSSPMIK (aa 594−648) was identified. Identified internal fragment ions are designated. In combination with automated Edman degradation (data not shown) this PSD fragment data allowed identification of the phosphorylated amino acid residue in the known primary structure.

Table 1: Sequence Analysis Results of hGab-1 Phosphopeptides[a]

amino acid sequence of identified phosphopeptides	$[M + H]^{+}$ [b]	aa in hGab-1[c]	phosphorylated residues	fraction[d]	part[e] of ^{32}P [%]
HGMNGFFQQQMI**Y**DSPPSR	2320.0	230−248	Y242	b/26, d/16	1.8
VSPSSTEADGEL**Y**VFNTPSGTSSVETQMR	3156.4	273−301	Y285	f/29	1.7
TASDTDSS**Y**CIPTAGMSPSR	2197.8	365−384	Y373	b/6	2.7
NVLTVGSVSSEELDEN**Y**VPMNPNSPPR	3024.4	431−457	Y447	h/12, g/19, c/59	27.6
QHSSSFTEPIQEAN**Y**VPMTPGTFDFSSFGMQ VPPPAHMGFR	4637.0	458−498	Y472	a/63, a/66−67, f/35−38	30.7
FPMSPRPDSVHSTTSSSDSHDSEEN**Y**VPMNPN LSSEDPNLFGSNSLDGGSSPMIK	6186.6	594−648	Y619	b/26, e/25−26, h/24−26, i/24	17.8
QVE**Y**LDLDLDSGK	1574.7	654−666	Y657	j/17−18	6.1
SSGSGSSVADERVD**Y**VVVDQQK	2392.1	675−696	Y689	d/16	11.6

[a] Tryptic peptides of hGab-1 were analyzed after anion exchange HPLC and reversed phase HPLC by mass spectrometry and Edman degradation. Phosphorylated tyrosine residues are marked in bold letters. [b] Single charged monoisotopic mass. [c] Numbering according to Lehr et al. (*1*). [d] Fractions from anion exchange chromatography (letters)/reversed phase (numbers) HPLC (see Figure 2B). [e] Total amount of radioactivity incorporated into the identified phosphopeptides corresponds to 100%.

residues are located in YXXM motifs exhibiting potential PI-3 kinase binding sites.

Approximately 12% of the identified radioactivity was obtained in a phosphopeptide (Y_{689}) containing no known potential binding motif for SH2 domain proteins. A second phosphopeptide (Y_{285}) also within another hydrophobic motif was only weakly phosphorylated (1.7%). Remaining phosphorylated peptides exhibited potential binding sites for signaling proteins containing SH2 domains such as Nck (Y_{242}), PLCγ (Y_{373}), and Syp (Y_{657}). These phosphopeptides contained 1.8−6.1% of the radioactivity found.

In summary, for IR-specific phosphorylation of hGab-1, we identified eight tyrosine phosphorylation sites (Table 1).

Functional Relevance of Tyrosine Residue Y447, Y472, and Y619 in hGab-1. For major phosphate incorporation, we identified the tyrosine residues located in potential PI-3 kinase binding sites. To elucidate the functional relevance of these IR-specific main phosphorylation sites, we investigated the ability of hGab-1 to interact with PI-3 kinase in a phosphorylation-dependent manner.

Therefore, we generated single, double, as well as triple mutants by changing each tyrosine residue within a NYVPM

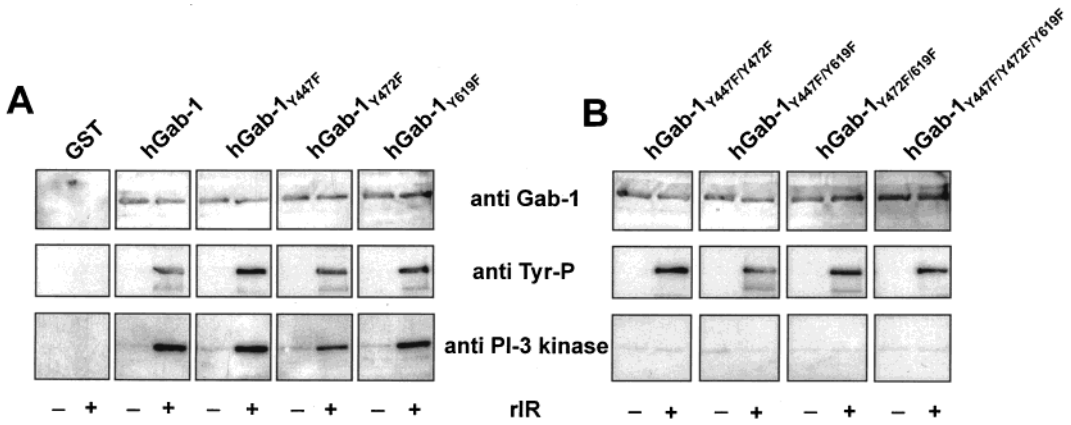

FIGURE 6: Binding of PI-3 kinase to hGab-1 in vitro. Comparison of GST-pull-down assays of wild-type hGab-1 and mutated variants. (A) Pull down assay of phosphorylated and nonphosphorylated wild-type hGab-1, single mutants (each 5 μg) and GST. Proteins were incubated with 1 mg of HepG2 cell lysates. The entire hGab-1 with bound proteins was recovered with glutathione beads (see Experimental Procedures). Aliquots of the precipitates were separated by SDS−PAGE and transferred to PVDF membranes. hGab-1, tyrosine phosphorylation, and PI-3 kinase (p85) were detected with specific antibodies. Lines describe absence (−) or presence (+) of named substances. Blots were initially probed with anti-PI-3 kinase and detection by BM Chemiluminescence (Boehringer) followed. Subsequently blots were stripped and reprobed with anti-Gab-1 and anti-αPtyr (RC20). (B) Pull down assay of phosphorylated and nonphosphorylated hGab-1 multiple mutants (each 5 μg). Pull down assays were performed as described above.

motif to phenylalanine. These hGab-1 mutants were used to perform GST pull down assays with lysates of human HepG2 cells in comparison to wild-type hGab-1 and GST in vitro.

Phosphorylated wild-type hGab-1 showed a substantial increase in PI-3 kinase binding in comparison to unphosphorylated hGab-1 (Figure 6). No binding of PI-3 kinase could be detected with GST alone as a control. For each single mutant of hGab-1, we observed an PI-3 kinase binding pattern identical to the wild-type protein (Figure 6A). Hence, changing only one tyrosine residue in NYVPM motifs showed no influence on the efficiency of phosphorylation-dependent protein interaction in comparison to the wild-type protein, but the phosphorylation dependent amplification of PI-3 kinase binding was completely abolished by changing a second tyrosine residue in a NYVPM motif (Figure 6B). Phosphorylation-dependent PI-3 kinase binding was also not observed by the triple mutant.

Stripping and reprobing blots with anti-Gab-1 antibodies proved equivalent amounts of hGab-1. To demonstrate tyrosine phosphorylation, blots were stripped again and reprobed with anti-phosphotyrosine antibodies. Phosphorylation of hGab-1 on tyrosine residues could only be detected after incubation with IR.

DISCUSSION

Gab-1 is activated and engaged in intracellular signaling of various RTKs, suggesting that the protein plays an important role in the generation of biological responses for various cytokines and growth factors (*3*−*7*, *25*, *26*). A wide spread set of biological responses are regulated by Gab-1, e.g., Gab-1 mediates branching and alveolar morphogenesis of epethelial cells via HGF receptor activation (*27*−*29*) and transformation of epithelial and NIH 3T3 cells (*30*, *31*, *6*). Furthermore, Gab-1 reduces the concentration of NGF required for inhibition of apoptosis via the three PI-3 kinase binding sites within Gab-1 (*3*).

Gab-1 contains several potential tyrosine phosphorylation sites, some of them situated in motifs that are thought to function as binding sites for SH2 domain containing proteins (*6*). As a result of structural and functional similarities, human Gab-1 appears to be a member of the multifunctional docking protein family consisting of IRS1−4 (*32*−*35*) and Gab-2 (*13*).

The shared usage of different IRS proteins by multiple receptors enables the integration of several receptor systems in a signaling complex (molecular cross-talk). On the other hand each receptor can engage multiple IRS proteins, which leads to a diversification of the regulated signaling pathways (*36*). Upon phosphorylation by various receptor-associated tyrosine kinases, certain IRS proteins might recruit different intracellular signaling proteins. For example, stimulation of IRS-1 phosphorylation by insulin leads to the association with the tyrosine phosphatase Syp. In contrast, no interaction of IRS-1 with Syp could be observed upon stimulation with interleukin 4 (IL4). Furthermore, no interaction of IRS-2 with Syp could be detected by stimulating cells with insulin or with IL4 (*36*). Additionally IRS-1 and IRS-2 do not bind phospholipase C_Y (*37*), whereas Gab-1 does (*6*). This leads to the hypothesis that differential and specific phosphorylation created by different RTKs might be the mechanism by which a intracellular adapter protein activates specific downstream pathways. Binding of a single cohort of SH2 domain proteins could be restricted by specific phosphorylation. Recently, we identified eight EGFR-specific tyrosine phosphorylation sites in hGab-1 (*1*). In this case, Y657 is the favored phosphorylation site and simultaneously a specific binding site of Syp.

To demonstrate the receptor-dependent specific phosphorylation pattern of hGab-1 by IR, we show that hGab-1 is a high affinity substrate of the IR and identified the main receptor specific tyrosine phosphorylation sites by MALDI mass spectrometry and automated Edman degradation.

Phosphorylation kinetics revealed that hGab-1 is a high affinity substrate for the IR (K_M: 12 μM); similar results were obtained when IR phosphorylation of human recombinant IRS-1 domain (aa: 586−1149, called hIRS-p30) was performed (*22*). In contrast, phosphorylation studies with synthetic peptides containing YXXM and YMXM motifs of IRS-1 resulted in K_M values between 24 to 300 μM (*38*). This indicates a complex substrate−receptor interaction of

hGab-1 with the IR and might depend on the intact structure of hGab-1 and IRS-1. Comparable results were achieved in a previous study using the EGFR (*1*).

IR phosphorylation of hGab-1 occurred exclusively on tyrosine residues. This substrate contains at least 17 potential tyrosine phosphorylation sites, including 11 binding sites for known SH2 domains enabling it to interact with PI-3 kinase, Grb2, phospholipase Cγ, Syp, and Crk (*1*, *6*, *7*). Tryptic digestion of hGab-1 generates 114 theoretical peptides. This amount increases when partial modifications (e.g., oxidation of Met) are expected. For effective separation of the phosphorylated tryptic hGab-1 peptides, we used a combination of two different successive HPLC protocols. Using MALDI-PSD-MS and peptide sequencing, we identified eight tyrosine residues that are phosphorylated by the IR (Table 1). Tyrosine residues Y_{447}, Y_{472}, and Y_{619} are within YXXM motifs (ENY_{447}VPMNPN, NY_{472}VPM, ENY_{619}-VPMNPN), which are predicted to bind to the SH2 domain in the 85-kDa regulatory subunit (p85) of the PI-3 kinase. These tyrosine residues represent the major phosphorylation sites specific for the IR. Tyrosine phosphorylation site Y_{242} exhibits sequence similarity according to PLCγ, Y_{373} to Nck, and Y_{657} to Syp binding sites (*39*, *40*). In contrast, identified phosphorylation sites including Y_{285}VFN and Y_{689}VVV are located in distinct hydrophobic motifs. Nevertheless, the probability exists that other tyrosine residues, in the vicinity of an aspartate or glutamate residue, may be phosphorylated. Such phosphorylated peptides could be represented by minor unidentified radiolabeled peaks of RP-HPLC.

The IR-specific hGab-1 phosphorylation displays a favorite phosphorylation of tyrosine residues in NYVPM motifs (Y_{447} 27.6%, Y_{472} 30.7, Y_{619} 17.7%). Overall, the part of incorporated radioactivity of these tyrosine residues in PI-3 kinase binding motifs exceeded 75%. Hence, tyrosine residues Y_{447}, Y_{472}, and Y_{619} represent the main tyrosine phosphorylation domain in the central part of hGab-1. In contrast, the other identified tyrosine residues (Y_{242}, Y_{373}, and Y_{657}) in known SH2 domain binding motifs were only slightly phosphorylated. Phosphorylation of the other five tyrosine residues located in known SH2 domain binding motifs could not be observed, indicating a high specificity of RTK-mediated phosphorylation.

Here we identified eight specific phosphorylation sites of hGab-1 for the IR. In comparison to this in a former investigation with the EGFR, we detected a nearly identical cohort of tyrosine phosphorylation sites in hGab-1 (*1*) (Figure 7). However, in contrast the quantitative distribution of phosphate incorporation catalyzed by EGFR is completely different. As the main EGFR phosphorylation site we identified tyrosine residue Y657 in the C-terminus of hGab-1 mediating a specific and efficient binding of Syp in vitro. Tyrosine residues situated in potential PI-3 kinase binding sites (YXXM) were only weakly phosphorylated. Our results for EGFR and IR suggest that a different qualitative phosphorylation of a common cohort of tyrosine residues plays a key role for generating signal selectivity at the molecular level.

To test the functional relevance of these results, GST pull down assays were performed. These investigations exhibited binding of PI-3 kinase in a phosphorylation-dependent manner catalyzed by the IR. We show that Y447, Y472, and Y619, which are postulated PI-3 kinase binding sites, in the central domain of hGab-1 are phosphorylated substantially and comparably by the IR. Following phosphorylation, these tyrosine residues mediate increased hGab-1 and PI-3 kinase interaction. Our results fit the observations of Holgado-Madruga et al. (*6*) who demonstrated that Gab-1 is the major binding partner of PI-3 kinase in 3T3L1 cells when stimulated with insulin. The same group also showed that Gab-1 has a major role in promoting cell survival by NGF engaging PI-3 kinase via the three YVPM motifs in in Gab-1 (*3*).

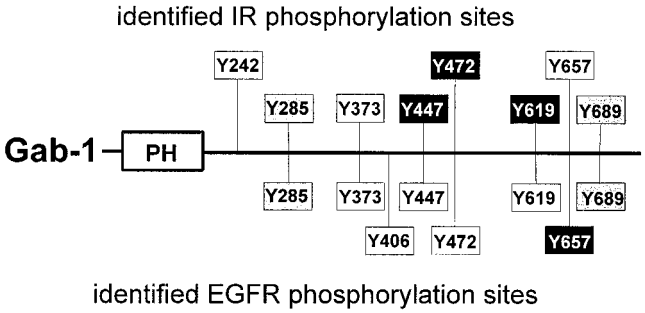

FIGURE 7: Receptor-specific tyrosine phosphorylation sites of hGab-1. Phosphorylation sites (for IR) identified (MALDI-PSD-MS and Edman sequencing) in this report are listed above the line. Tyrosine residues that correspond to phosphorylation sites in known binding motifs for SH2 domain proteins are shown as white boxes, whereas sites without known binding motifs for SH2 domain proteins are shown as gray boxes. Our recently identified tyrosine residues (*1*) specific for EGFR phosphorylation are listed below the line. The proclaimed specific predominant phosphorylation site for each receptor tyrosine kinase is displayed in black boxes.

Pull down assays with wild-type hGab-1 as well as different single, double, and triple mutants reveal that changing of one arbitrary tyrosine residue in a YVPM motive has no influence on binding efficiency of hGab-1 to PI-3 kinase. However, destroying a second putative PI-3 kinase binding motive abolishes phosphorylation-dependent interaction completely, which is also the case for the triple mutant. Binding of PI-3 kinase seems to depend on the number of phosphorylated residues rather than on its location. Bivalent interaction of hGab-1 via two of the three equally phosphorylated YVPM motifs is required for effective and specific binding. This is consistent with observations of Rordorf-Nikolic et al. (*41*) who demonstrated that full activation of PI-3 kinase by IRS-1 binding requires an interaction via both PI-3 kinase SH2 domains. In contrast to our observations with human IR, Rocchi et al. (*42*) described in a modified yeast two hybrid system, that PI-3 kinase interacts mainly with Y472 of hGab-1. Tyrosine Y447 as well as Y619 are participating in this process marginally.

In summary, our results suggest that hGab-1 is phosphorylated by various receptor tyrosine kinases i.e., IR and EGFR, on a common cohort of tyrosine residues but with completely different efficiencies. Analogous differences may also occur during interaction with other receptors, e.g., PDGF or HGF, and describe a molecular basis for signaling selectivity. Specific phosphorylation by different receptor tyrosine kinases could modulate binding of downstream signaling proteins and play a crucial role in the determination of signaling specificity. The underlying mechanism might be preferential binding of different receptor-specific SH2 domain proteins. Further investigations including other receptor tyrosine kinases and IRS proteins as well as studies in vivo will prove this hypothesis.

ACKNOWLEDGMENT

We thank G. Becker and H. Korte for technical assistance, G. Roth for helpful discussion, and J. Gillette for critical reading of the manuscript.

REFERENCES

1. Lehr, S., Kotzka, J., Herkner, A., Klein, E., Siethoff, C., Knebel, B., Noelle, V., Brüning, J. C., Klein, H. W., Meyer, H. E., Krone, W., and Müller-Wieland, D. (1999) *Biochemistry 38*, 151−159.
2. Seedorf, K. (1995) *Metabolism 44*, 24−32.
3. Holgado-Madruga, M., Moscatello, D. K., Emlet, D. R., Dietrerich, R., and Wong, A. J. (1997) *Proc. Natl. Acad. Sci. U.S.A. 94*, 12419−12424.
4. Ong, S. H., Lim, Y. P., Low B. C., and Guy G. R. (1997) *Biochem. Biophys. Res. Commun. 238*, 261−266.
5. Nguyen, L., Holgado-Madruga, M., Maroun, C., Fixman, E. D., Kamikura, D., Fournier, T., Charest, A., Tremblay, M. L., Wong, A. J., and Park, M. (1997) *J. Biol. Chem. 272*, 20811−20819.
6. Holgado-Madruga, M., Emlet, D. R., Moscatello, D. K., Godwin, A. K., and Wong, A. J. (1996) *Nature 397*, 560−564.
7. Nishida, K., Yoshida, Y., Itoh, M., Fukada, T., Ohtani, T., Shirogane, T., Atsumi, T., Takahashi-Tezuka, M., Ishihara, K., Hibi, M., and Hirano, T. (1999) *Blood 93*, 1809−1816.
8. Snider, W. D. (1994) *Cell 77*, 627−638.
9. Zarnegar, R., and Michalopoulos, G. K. (1995) *J. Cell Biol. 129*, 1177−1180.
10. Brinkmann, V., Foroutan, H., Sachs, M., Weidner, K. M., and Birchmeier, W. (1995) *J. Cell Biol. 131*, 1573−1586.
11. Garcia-Ocana, A., Takane, K. K., Syed, M. A., Philbrick, W. M., Vasavada, R. C., and Stewart, A. F. (2000) *J. Biol. Chem. 275*, 1226−1232.
12. Yenush, L., and White, M. F. (1997) *Bioassays 19*, 491−500.
13. Gu, H., Pratt, J. C., Burakoff, S. J., and Neel, B. G. (1998) *Mol. Cell 2*, 729−740.
14. Kasuga, M., White, M. F., and Kahn, C. R. (1985*) Methods Enzymol. 109*, 609−621.
15. Laemmli, U. K. (1970) *Nature 277*, 680−685.
16. Rosenfeld, J., Capdevielle, J., Guillemont, J. C., and Ferrara, P. (1992) *Anal. Biochem. 203*, 173−179.
17. Hellmann, U., Wernstedt, C., Gonez, J., and Heldin, C. H. (1995) *Anal. Biochem. 224*, 451−455.
18. Meyer, H. E., Hoffmann-Posorske, E., Donella-Deana, A., and Korte, H. (1991) *Methods Enzymol. 201*, 206−224.
19. Eng, J., McCormack, A. L., and Yates, J. R., III. (1994) *Am. Soc. Mass Spectrom. 5*, 976−989.
20. Yates, J. R., III, Eng, J., McCormack, A., and Schieltz, D. (1995) *Anal. Chem. 67*, 1426−1436.
21. Towbin, H., Staehlin, T., and Gordon, J. (1979) *Proc. Natl. Acad. Sci. U.S.A. 76*, 4350−4354.
22. Siemeister, G., al-Hasani, H., Klein, H. W., Kellner, S., Streicher, R., Krone, W., and Müller-Wieland, D. (1995) *J. Biol. Chem. 270*, 4870−4874.
23. Kohanski, R. A. (1993) *Biochemistry 32*, 5766−5772.
24. Wei, L., Hubbard, S. R., Hendrickson, W. A., and Ellis, L. (1995) *J. Biol. Chem. 270*, 8122−8130.
25. Daub, H., Wallasch, C., Lankenau, A., Herrlich, A., and Ullrich, A. (1997) *EMBO J. 16*, 7032−7044.
26. Korhonen J. M., Said F. A., Wong A. J., and Kaplan D. R. (1999) *J. Biol. Chem.* 274, 37307−37314.
27. Weidner, K. M., Di Cesare, S., Sachs, M., Brinkmann, V., Behrens, J., and Birchmeier, W. (1996) *Nature 384*, 173−176.
28. Niemann, C., Brinkmann, V., Spitzer, E., Hartmann, G., Sachs, M., Naundorf, H., and Birchmeier, W. (1998) *J. Cell Biol. 143*, 533−545.
29. Maroun, C. R., Holgado-Madruga, M., Royal, I., Naujokas, M. A., Fournier, T. M., Wong, A. J., and Park, M. (1999) *Mol. Cell Biol. 19*, 1784−1799.
30. Fixman, E. D., Holgado-Madruga, M., Nguyen, L., Kamikura, D., Fournier, T., Wong, A. J., and Park, M. (1997) *J. Biol. Chem. 272*, 20167−20172.
31. Bardelli, A., Longati, P., Williams, T. A., Benvenuti, S., and Comoglio, P. M. (1999) *J. Biol. Chem. 274*, 29274−29281.
32. Sun, X. J., Rothenberg, P., Kahn, C. R., Backer, J. M., Araki, E., Wilden, P. A., Cahill, D. A., Goldstein, B. J., and White, M. F. (1991) *Nature 352*, 73−77.
33. Sun, X. J., Wang, L.-M., Zhang, Y., Yenush, L., Myers, M. G., Jr., Glasheen, E., Lane, W. S., Pierce, J. H., and White, M. F. (1995) *Nature 377*, 173−177.
34. Lavan, B. E., Lane, W. S., and Lienhard, G. E. (1997) *J. Biol. Chem. 272*, 11439−11443.
35. Lavan, B. E., Fantin, V. R., Chang, E. T., Lane, W. S., Keller, S. R., and Lienhard, G. E. (1997) *J. Biol. Chem. 272*, 21403-21407.
36. Sun, X. J., Pons, S., Wang, L. M., Zhang, Y., Yenush, L., Burks, D., Myers, M. G., Jr., Glasheen, E., Copeland, N. G., Jenkins, N. A., Pierce, J. H., and White, M. F. (1997*) Mol. Endocrinol. 11*, 251−262.
37. Myers, M. G., Jr., Sun, X. J., Cheatham, B., Jachna, B. R., Glasheen, E. M., Backer, J. M., and White, M. F. (1993) *Endocrinology 132*, 1421−1430.
38. Shoelson, S. E., Chatterjee, S., Chaudhuri, M., and White, M. F. (1992) *Proc. Natl. Acad. Sci. U.S.A. 89*, 2027−2031.
39. Songyang, Z., Shoelson, S. E., McGlade, J., Olivier, P., Pawson, T., Bustelo, X. R., Barbacid, M., Sabe, H., Hanafusa, H., and Yi, T. (1994) *Mol. Cell. Biol. 14*, 2777−2785.
40. Songyang, Z., Shoelson, S. E., Chaudhuri, M., Gish, G., Pawson, T., Haser, W. G., King, F., Roberts, T., Ratnofsky, S., and Lechleider, R. J. (1993) *Cell 72*, 767−778.
41. Rordorf-Nikolic, T., Van Horn, D. J., Chen, D., White, M. F., and Backer, J. M. (1995*) J. Biol. Chem. 270*, 3662−3666.
42. Rocchi, S., Tartare-Deckert, S., Murdaca, J., Holgado-Madruga, M., Wong, A. J., and Van Obberghen, E. (1998) *Mol. Endocrinol. 12*, 914−923.

BI000982K